



# INFLUENCE OF THE FERROMAGNETIC COMPONENT ON THE MAGNETIC PROPERTIES OF POLYMER-MATRIX SOFT MAGNETIC COMPOSITES

Zuzana Birčáková, Peter Kollár, Ján Fúzer, Magdalena Streckova, Juraj Szabó, Radovan Bureš, Mária Fáberová

## Abstract

*The paper presents the study of the influence of different ferromagnetic powders on magnetic properties of polymer-matrix soft magnetic composites. Samples were prepared from pure Fe and Permalloy powders with the same amount of resin and by the same technological process. The coercivity, the real part of complex permeability, saturation magnetic polarization, hysteresis loops and total energy losses and their components were investigated. It was found that the coercivity, DC losses, classical losses, excess losses and thus the total energy losses of composites depended on intrinsic magnetic properties and/or on the size and shape of ferromagnetic powder particles, while the permeability of composites was affected predominantly by inner demagnetizing fields due to the insulation. The numbers of moving domain walls involved in magnetization reversal were analyzed in connection with the magnetic properties.*

**Keywords:** *soft magnetic composite, iron powder, Permalloy, magnetic properties, energy losses, hysteresis loop*

## INTRODUCTION

Soft magnetic materials are the kind of materials which can be magnetized and demagnetized easily. They exhibit low coercivity, less than 1000 A/m down to so far the least achieved ~0.16 A/m and their typical use covers applications with time-varying magnetic flux [1-3]. The following properties are required for soft magnetic materials: high permeability, low coercivity, high saturation magnetic polarization, low energy losses at DC magnetization, high specific electrical resistivity in order to minimize classical losses (caused by eddy currents flow induced in conductive material with time change of magnetic flux) and thus low total energy losses during AC magnetization [1-4].

A typical soft magnetic material is iron, characterized by high saturation polarization ~2.15 T [2]. By adding various elements to Fe, it is possible to improve certain properties of the material, thus forming Fe-alloys that may contain e.g. Al, Si, Cr, Nb, Mo, Ni or Co [4]. For example, FeSi alloys are the most widespread in terms of use, mostly for AC applications at frequency 50-60 Hz, due to the positive effect of Si addition on the electrical resistivity increase. CoFe alloys show the highest saturation polarization of all known alloys (2.46 T). NiFe alloys are used at a wide range of compositions from 30 to 80 wt. % of Ni, varying the properties. Those with high Ni content (also called Permalloys) provide very high permeability (up to 300,000) and very low coercivity as well, but at the expense of the saturation polarization decrease [2,3].

The development of new materials still continues with the aim of achieving excellent magnetic properties for specific applications. The new soft magnetic materials available in recent decades include besides the nanocrystalline or the amorphous alloys also the materials prepared by compaction of ferromagnetic powders and the soft magnetic composites [1-4].

Soft magnetic composite materials (SMCs) are made of soft magnetic powders coated with a layer of electrically insulating film. They provide competitive soft magnetic properties and several advantages over traditional materials, such as high electrical resistivity leading to low classical and total energy losses at medium to higher frequencies, 3D magnetic flux and isotropic physical properties [4,5]. SMCs cover the region of electromagnetic applications in alternating magnetic fields where traditional materials cannot be used, because in electrical steel sheets total core losses rise rapidly with the increasing frequency (above  $\sim 100$  Hz), and on the other hand, soft ferrites have low saturation magnetic polarization, thus SMCs are well suited for use as cores for medium to higher frequency ( $\sim$  kHz -  $\sim$  MHz range) transformers and electromotors, electromagnetic circuits, sensors, electromagnetic actuation devices, frequency filters, induction field coils, magnetic seal systems and magnetic field shielding [4-6]. They are produced by the powder metallurgy techniques offering a wide range of complex shape design of the products. Their properties can be tuned in different ways by the composition (e.g. type and percentage of ferromagnetic and insulating components, size and shape of powder particles) as well as by the processing parameters (e.g. pressure, temperature, time or atmosphere during the compaction and heat treatment), and while some of these factors significantly affect the properties of the resulting SMC, others less so [5,6].

One of the most important characteristics of magnetic materials is the total energy dissipated during the magnetization reversal, causing the heating of devices. Therefore the effort is to minimize the losses as much as possible. The energy losses come from irreversible mechanisms of the magnetization process, specifically from eddy currents induced by the magnetic induction changes accompanying those mechanisms [3,5,7]. It is useful to express total losses mathematically and so various models exist [7-9], e.g. G. Bertotti's one, where he found that excess losses are related to numbers of active magnetic objects (simultaneously moving domain walls) [7].

The aim of this work is to investigate the influence of different soft ferromagnetic powders (Fe and Permalloy) on the magnetic properties of polymer-matrix soft magnetic composites, as the coercivity, the real part of complex permeability, saturation magnetic polarization and total energy losses. The total losses will be separated into DC, classical and excess loss components and numbers of active magnetic objects will be calculated.

## EXPERIMENTAL

Two samples of polymer-matrix SMCs were chosen for comparison. As a ferromagnetic part for the first sample the Permalloy powder (from producer JSC Tula, Russia) was used, prepared by atomization of melt alloy, hence containing smooth spherical particles. The size range of Permalloy particles was from  $35 \mu\text{m}$  to  $105 \mu\text{m}$  and the average size was  $\approx 64 \mu\text{m}$ , measured by laser diffraction granulometer [10]. As a ferromagnetic part for the second sample the iron powder Fe ABC 100.30 (from producer Höganäs AB, Sweden) was used, containing particles of irregular shape with size ranging from  $10 \mu\text{m}$  to  $210 \mu\text{m}$ , the average size was  $\approx 100 \mu\text{m}$  (measured by laser diffraction granulometer). As an insulation the boron modified phenolic resin (PFRB) was applied, its synthesis was reported in [11]. SMCs with  $(20 \pm 1)$  vol. % of PFRB resin were prepared in the form of a ring (outer diameter  $\approx 24$  mm, inner diameter  $\approx 18$  mm, height  $\approx 2$  mm) by compacting at

uniaxial pressure 600 MPa followed by heat curing up to the temperature 220 °C (step 1.5 °C/min) in air atmosphere [10,12]. Samples are labelled “SMC Permalloy-PFRB” and “SMC Fe-PFRB” (in previous works as “P-PFRB” [10] and “Fe79%” [12], respectively, where their basic properties can also be found). Both samples have the porosity of (5±1) %, the volume fraction of ferromagnetic component of ≈ 75 % and the specific electrical resistivity of  $(8\pm 3) \cdot 10^{-3} \Omega\text{m}$ , and their structure documentation by scanning electron microscopy is in Fig.5(a,b) in [10] and in Fig.2(d) in [12], showing good insulation of ferromagnetic particles. For comparison, the compacted (800 MPa) and sintered (1200 °C, 1 h, Ar) pure Permalloy and Fe powder ring-shaped samples were also prepared.

The coercivity was measured by Foerster Koerzimat 1.097 HCJ. The total energy losses were obtained from the AC hysteresis loops measured at maximum magnetic induction 0.1 T (in ferromagnetic material) in the frequency range from 100 Hz to 20 kHz by the AC hysteresisgraphs MATS-2010M and MATS-2010SA. Similarly the DC energy losses were found from the DC hysteresis loops measured by the DC fluxmeter-based hysteresisgraph. The real part of complex relative permeability was measured in the frequency range from 100 Hz to 40 MHz by the impedance analyzer HP 4194A (in the configuration of two terminal connection).

## RESULTS AND DISCUSSION

In Fig. 1 the real part of complex relative permeability of the compacted and sintered Permalloy and iron powder and of the investigated SMCs (in the inset [10,12]) is depicted as a function of frequency  $f$  in the range from 100 Hz to 40 MHz. We can see that the heat treated powder compacts exhibit very high difference in the values at the beginning of the measured dependence (at  $f = 100$  Hz), but in the case of the SMC samples these values are almost the same. In both the powder compacts the magnetization reversal is facilitated as the more effective heat treatment (with higher temperature of sintering) led to the release of internal stresses and thus less pinning sites for the moving domain walls, but the difference in the ferromagnets is significant. On the other hand, the absolute values for SMC samples are lowered due to the content of insulation as well as the less effective heat treatment, but their difference is negligible. It can be explained in terms of inner demagnetizing fields, coming from the magnetic poles of insulated ferromagnetic particles [2,5,13] in SMC, which weaken the magnetic interactions between ferromagnetic particles and the magnetic flux is cut off. The intensity of inner demagnetizing fields was found to increase with the increasing non-magnetic content (insulation + porosity) [5,13] and the influence of these fields on the permeability of SMC (with non-magnetic matrix) becomes dominant even at very low non-magnetic content (from more than about 10 vol.% the influence of the intrinsic permeability of ferromagnet becomes negligible) [14].

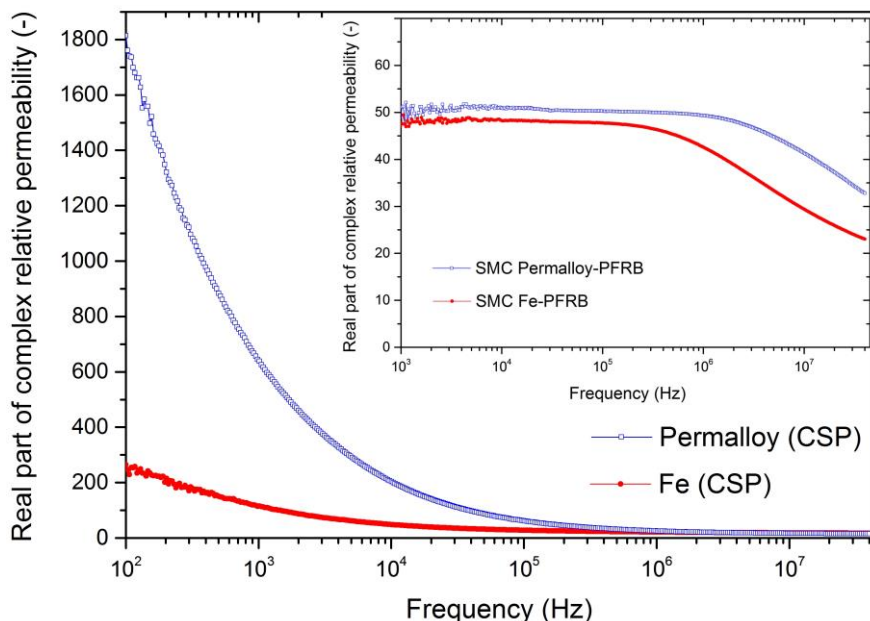


Fig. 1. Real part of complex relative permeability as a function of frequency of the Permalloy and iron compacted and sintered powder (CSP) and of the investigated SMC samples (inset [10,12])

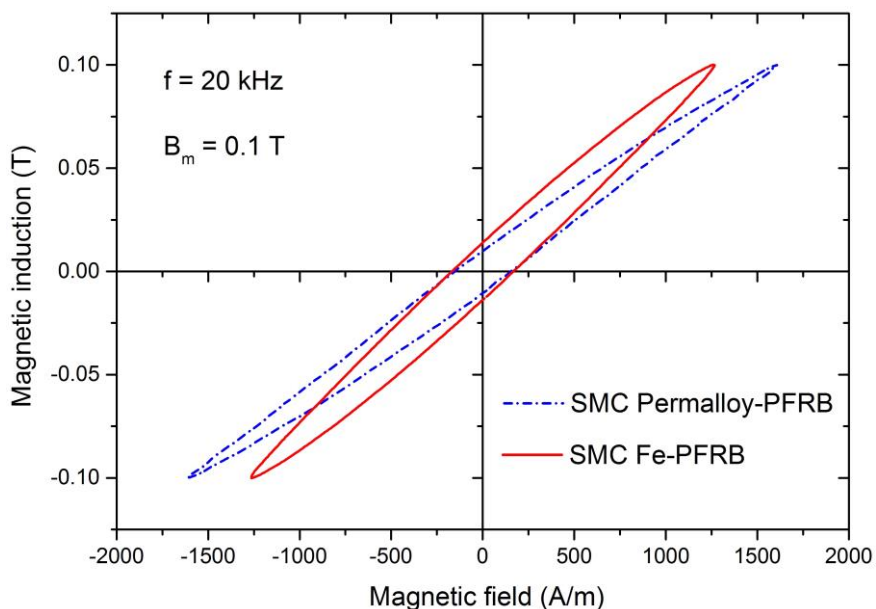


Fig. 2. Hysteresis loops of the investigated SMC samples at maximum induction 0.1 T and frequency 20 kHz

In Fig. 2 the hysteresis loops of the investigated SMC samples at frequency 20 kHz and maximum induction  $B_m$  0.1 T are shown. We can see that the slope of the loop (corresponding to peak permeability  $\mu_{peak}$ ) is even slightly higher for sample SMC Fe-PFRB (meaning higher  $\mu_{peak}$  at 0.1 T), which is in agreement with the total permeability measurements having similar dependences (in [10,12] the maximum total relative permeability was investigated). Besides the strong influence of inner demagnetizing fields, the slightly higher  $\mu_{peak}$  of SMC Fe-PFRB can be explained by the different initial magnetization curve (at which the peak of the hysteresis loop lies) due to the different saturation magnetic polarization  $J_S$  of SMC. The values were calculated from relation [15]

$$J_S = J_{S(ferro)} C, \quad (1)$$

where  $C$  is the filling factor  $\approx 0.75$  (volume fraction of ferromagnetic component / 100 %) and  $J_{S(ferro)}$  is the saturation magnetic polarization of the ferromagnet (sintered compact as well as pure powder) [2]. Values of  $J_S$  are in Tab. 1.

Tab. 1 Saturation magnetic polarization and coercivity of ferromagnets and SMC samples

Material	Permalloy sintered compact	Permalloy powder	SMC Permalloy -PFRB	Fe sintered compact	Fe powder	SMC Fe-PFRB
Saturation magnetic polarization $J_S$ [T]	0.8	0.8	0.6	2.15	2.15	1.6
Coercivity $H_C$ [A/m]	15	180	310	190	290	470

The coercivity  $H_C$  of material depends on the amount of pinning sites for moving domain walls as well, i.e. structural defects such as dislocations, inclusions, voids, impurities, grain boundaries, surface roughness or internal stresses, but unlike the permeability it does not depend on inner demagnetizing fields [2-5]. Hence the values measured for SMC samples (Tab. 1, [10,12]) are reflected by the influence of the values of ferromagnets (the sintered compacts and the pure powders, Tab. 1).

The total energy losses  $W_{tot}$  of the investigated SMC samples measured in the frequency range from 100 Hz to 20 kHz at  $B_m$  0.1 T were separated into the DC losses  $W_{DC}$ , the classical losses  $W_{cl}$  and the excess losses  $W_{exc}$  according to the well-known concept of separation [3-5,7,9], Fig. 3. We can observe higher  $W_{DC}$  for the sample SMC Fe-PFRB, because  $W_{DC}$  depend on the same factors as  $H_C$  and thus correlate with its values [5]. For small sample cross-section (less than  $5 \times 5 \text{ mm}^2$ ) only the intra-particle eddy currents are present [9]. The contribution of the intra-particle classical losses  $W_{cl-intra}$  per time period  $T$  can be calculated based on Faraday's law:

$$W_{cl-intra} = \int_0^T \frac{K(R) S_k}{\rho_R} \left( \frac{dB}{dt} \right)^2 dt, \quad (2)$$

where  $\rho_R$  is the specific electrical resistivity of ferromagnet,  $(dB/dt)$  is the time change of magnetic induction and  $K(R)$  is the function defined for equivalent rectangular ferromagnetic particles with cross-sectional area  $S_k$  and aspect ratio  $R = \text{height/width}$  of

rectangle [9]. If the average magnetic induction rate is assumed,  $(dB/dt) = 4 B_m f$ , and the same symmetrical square shape particles are approximated,  $R = 1$ ,  $K(R) \approx 0.0345$  and  $S_k = \pi d^2/4$  (where  $d$  is the average diameter of particles), the relation (2) becomes [9]:

$$W_{cl-intra} \approx (0.433 d^2 B_m^2 f) / \rho_R \quad (3)$$

In Fig. 3 we can observe that  $W_{cl-intra}$  (calculated from Eq. (3)) increase more steeply in the case of sample SMC Fe-PFRB, because of the larger average particle size for the eddy currents. The calculation does not consider particle agglomeration, and hence the absolute values of  $W_{cl-intra}$  are the lowest limit for ideally insulated particles. The excess losses  $W_{exc}$  were obtained as a difference:

$$W_{exc} = W_{tot} - W_{DC} - W_{cl-intra} \quad (4)$$

G. Bertotti found that  $W_{exc}$  are directly related to the numbers of active magnetic objects (MOs) involved in magnetization reversal and can be expressed in terms of the excess field  $H_{exc}$  acting on MOs [7]. When there are  $n$  active MOs present in the cross-section of magnetic material  $S$  (for SMC the sum of all ferromagnetic particles cross-sections),  $H_{exc} \sim (dB/dt) / n$ , and considering average magnetic induction rate  $(dB/dt) = 4 B_m f$ , it leads to the relations [7]:

$$n = (16 G S B_m^2 f) / (W_{exc} \rho_R), \quad (5)$$

(coefficient  $G = 0.1356$ ), and

$$H_{exc} = W_{exc} / (4 B_m) \quad (6)$$

In Fig. 4 the numbers of active MOs  $n$  in cross-section of the investigated SMC samples (calculated from Eq. (5)) are plotted as a function of  $H_{exc}$  and  $f$  (inset) at  $B_m$  0.1 T. We can observe that sample SMC Permalloy-PFRB contains higher numbers  $n$  than sample SMC Fe-PFRB, which is reflected by lower  $W_{exc}$  (Fig. 3). Higher  $n$  are due to better intrinsic soft magnetic properties (such as higher permeability and lower coercivity) of the ferromagnetic component in SMC Permalloy-PFRB, thus the values of  $n$  for this sample with 20 vol. % of resin are comparable with Fe-based SMC with 7 vol. % of resin [16]. The values of  $n$  found for sample SMC Fe-PFRB are similar to the ones for FeSi-based SMC with the same amount of resin [17]. Finally, the sample SMC Permalloy-PFRB exhibits lower  $W_{tot}$  (Fig. 3), which is also visible from the slightly smaller area of its hysteresis loop (Fig. 2).

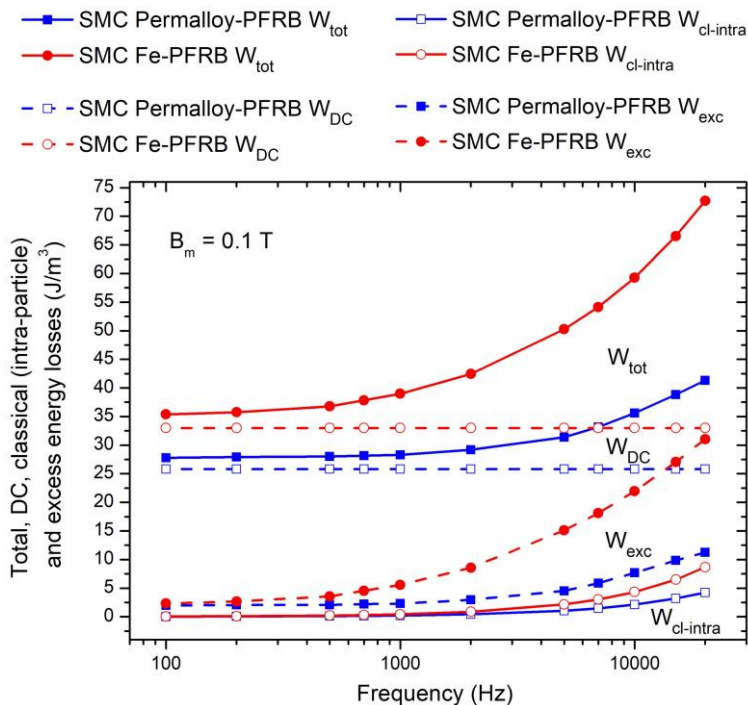


Fig. 3. Separation of total energy losses into DC, classical (intra-particle) and excess losses of the investigated SMC samples as a function of frequency at maximum induction 0.1 T.

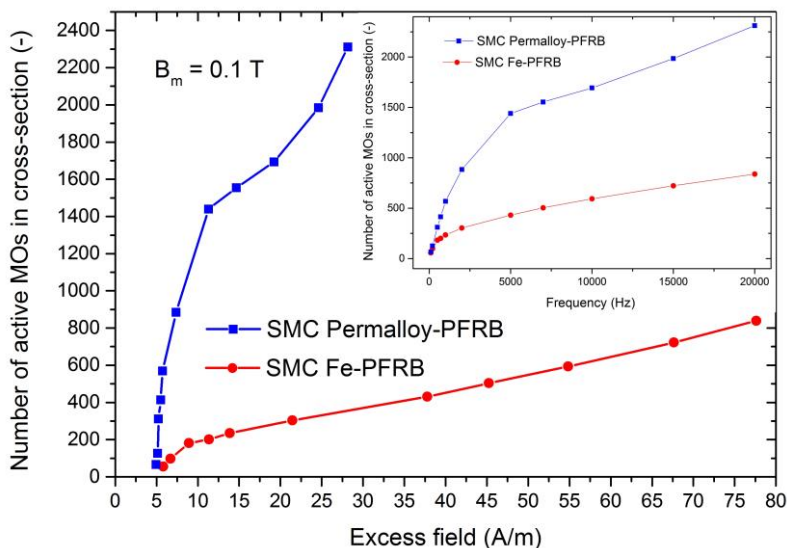


Fig. 4. Numbers of active MOs in cross-section of the investigated SMC samples as a function of excess field and of frequency (inset) at maximum induction 0.1

## CONCLUSION

In this work we investigated the polymer-matrix soft magnetic composite materials differing in the ferromagnetic component (pure Fe and Permalloy powders were used). A significant influence of the intrinsic magnetic properties as well as of the size and shape of ferromagnetic powder particles on the resulting coercivity, DC losses, classical losses, excess losses and the total energy losses of the prepared composites was found, depending on the numbers of moving domain walls involved in magnetization reversal (except for classical losses). The much lower coercivity was confirmed for the compacted and sintered powder of Permalloy compared to Fe, which has reflected in the lower coercivity, DC losses and excess losses of the Permalloy-based composite. Together with the lower intra-particle classical losses due to smaller average particle size, the Permalloy-based composite sample exhibited also lower total energy losses. The calculated numbers of active magnetic objects (moving domain walls) were higher as they are inversely proportional to excess losses, meaning the magnetization reversal is facilitated. Saturation magnetic polarization was higher for the Fe-based composite due to its higher value for iron compared to Permalloy. On the other hand, the real part of complex permeability and the peak permeability of composites were influenced predominantly by inner demagnetizing fields given by the level of particle insulation. Although the real part of complex permeability at frequency 100 Hz was for the compacted and sintered Permalloy powder higher by ~ 85 % than for the compacted and sintered iron powder, these values were in the case of composite samples almost identical.

## ACKNOWLEDGEMENT

This work was realized within the frame of the project “FUCO” financed by Slovak Research and Development Agency under the contract APVV-20-0072; and by Scientific Grant Agency of Ministry of Education of Slovak Republic and Slovak Academy of Science — projects VEGA 1/0143/20, VEGA 1/0225/20 and VEGA 2/0029/21. This work was also supported by the Development Operational Program Research and Innovation for the project “New unconventional magnetic materials for applications“, ITMS: 313011T544, co-funded by the European Regional Development Fund.

## REFERENCES

- [1] Jiles, D.: *Acta Mater.* vol. 51, 5907, 2003.
- [2] Tumanski, S.: *Handbook of magnetic measurements*, CRC Press - Taylor & Francis Group, Boca Raton, 2011.
- [3] Coey, JMD.: *Magnetism and magnetic materials*, Cambridge University Press, 2009.
- [4] Buschow, KHJ.: *Concise encyclopedia of magnetic and superconducting materials*, Elsevier, Oxford, UK, 2005.
- [5] Périgo, EA., Weidenfeller, B., Kollár, P., Füzér, J.: *Appl. Phys. Rev.*, vol. 5, 031301, 2018, p. 37.
- [6] Sunday, KJ, Taheri, ML.: *Metal Powd. Rep.*, vol. 72, no. 6, 2017.
- [7] Bertotti, G.: *IEEE Trans. Magn.*, vol. 24, 1988621, p. 630.
- [8] Landgraf, FJG, de Campos, MF., Leicht, J.: *J. Magn. Magn. Mater.*, vol. 320, 2008, p. 2494.
- [9] de la Barrière, O., Appino, C., Fiorillo, F., Ragusa, C., Lecrivain, M., Rocchino, L., Ben Ahmed, H., Gabsi, M., Mazaleyrat, F., LoBue, M.: *IEEE Trans. Magn.*, vol. 49, 2013, p. 1318.
- [10] Strečková, M., Szabó, J., Baťko, I., Baťková, M., Birčáková, Z., Füzér, J., Kollár, P.,

- Kovalčíková, A., Bureš, R., Medvecký, L.: Bull. Mater. Sci., vol. 43, no. 1, art. no. 37, 2020.
- [11] Strečková, M., Bureš, R., Fáberová, M., Medvecký, L., Füzér, J., Kollár, P.: Chinese J. Chem. Eng., vol. 23, 2015, p. 736.
- [12] Birčáková, Z., Füzér, J., Kollár, P., Szabó, J., Jakubčín, M., Strečkova, M., Bureš, R., Fáberová, M.: J. Alloys Compd., vol. 828, 2020, p. 154416.
- [13] Mattei, JL., Le Floch, M.: J. Magn. Magn. Mater., vol. 257, 2003, p. 335.
- [14] Pittini-Yamada, Y., Périgo, EA., de Hazan, Y., Nakahara, S.: Acta Mater., vol. 59, , 2011, p.4291.
- [15] Anhalt, M., Weidenfeller, B.: J. Appl. Phys., vol. 105, 2009, p. 113903.
- [16] Birčáková, Z., Füzér, J., Kollár, P., M. Strečkova, Strečková, M., Bureš, R., Fáberová, M.: J. Magn. Magn. Mater., vol. 485, 2019, p. 1.
- [17] Ďáková, L., Füzér, J., Dobák, S., Kollár, P., Osadchuk, Y., Strečková, M., Fáberová, M., Bureš, R., Kurek, P., Vojtko, M.: IEEE Trans. Magn., vol. 54, no. 12, 2018, p. 2003206.



# IRON BASED SOFT MAGNETIC COMPOSITE MATERIAL PREPARED BY INJECTION MOLDING

Zuzana Birčáková, Peter Kollár, Bernd Weidenfeller, Ján Fúzer, Radovan Bureš, Mária Fáberová

## **Abstract**

*Soft magnetic composite materials consisting of FeSi powder and polypropylene were prepared by the injection molding method, with different polypropylene contents of 25, 30 and 35 vol. %. The magnetic and electrical properties as well as the structure of the composites were investigated. The samples exhibited very low porosity, high electrical resistivity, relatively low coercivity, sufficient saturation magnetic flux density and permeability, and high resonant frequency. FeSi particles were found to be well insulated from each other and homogeneously dispersed in the polymer matrix of the composite. The observed isotropic structure was confirmed by the fitting of the experimental dependence with the analytical expression of the reversible relative permeability vs. magnetic flux density.*

**Keywords:** *soft magnetic composite, injection molding, magnetic properties, reversible permeability, initial magnetization curve*

## **INTRODUCTION**

Soft magnetic composite materials (SMCs) represent a kind of soft magnetic material with a still increasing significance in electromagnetic applications. They are composed of ferromagnetic particles electrically insulated from each other [1-5]. The insulation binders and coatings can be organic and inorganic and their mixtures, the organic ones are various epoxy resins, acrylic, polyurethane and polyester powders or their hybrids, and the inorganic ones can be sulphates, phosphates, ceramics or soft magnetic ferrites [5]. SMCs provide 3-D isotropic behaviour of physical properties, the reduction of eddy current losses leading to low total energy losses at medium to higher frequencies ( $\geq 100$  Hz up to  $\sim$  MHz), relatively high saturation induction and magnetic permeability and relatively low coercivity. SMCs find use in a wide range of applications as such electric motors, generators, transformers or sensors [1-5].

In powder metallurgy there are four main manufacturing techniques of polymer-bonded composite production: calendaring, injection molding, extrusion, and compression bonding by a press [1]. Although the last one is the most frequently used, the others offer various advantages as well.

---

Zuzana Birčáková, Radovan Bureš, Mária Fáberová: Institute of Materials Research, Slovak Academy of Sciences, Watsonova 47, 04001 Košice, Slovakia  
Peter Kollár: Institute of Physics, Faculty of Science, P.J. Šafárik University, Park Angelinum 9, 04154 Košice, Slovakia  
Bernd Weidenfeller: Institute of Electrochemistry, Technical University of Clausthal, Arnold-Sommerfeld-Str. 6, 38678 Clausthal-Zellerfeld, Germany

The injection molding (IM) process involves forcing the heated mixture of ferromagnetic powder and thermoplastic binder via tubes into a mold where it is allowed to cool and harden [1]. SMCs prepared by the IM method were investigated in works e.g. [6-9].

The aim of this work was to prepare soft magnetic composite materials composed of FeSi powder and polypropylene with different volume content and to investigate their magnetic and electrical properties.

## EXPERIMENTAL

The particle size distribution of FeSi powder was examined by laser diffraction granulometer. The microstructure of the samples was observed with Olympus GX71 light optical microscope (LOM) and TESLA BS 340 scanning electron microscope (SEM). Specific electrical resistivity was investigated by the four probe method using Mitsubishi Loresta AX. The coercivity was measured by Foerster Koerzimat 1.097 HCJ on cylinder-shaped samples. The initial magnetization curves were recorded by the DC fluxmeter-based hysteresisgraph ([11]) on ring-shaped samples, in order to obtain the maximum total relative permeability. The initial relative permeability and the resonant frequency were measured by the Impedance Analyzer HP 4294A (40 Hz - 110 MHz). The reversible relative permeability was measured by the setup based on the lock-in amplifier reading of the induced voltage ([11]), on ring-shaped samples, at the frequency 200 Hz.

## MATERIAL PREPARATION AND CHARACTERIZATION

Soft magnetic composite samples composed of FeSi powder and polypropylene were prepared by the IM method. FeSi powder with Si content of 6.8 wt. % (from producer Höganäs AB Sweden [10]) was chosen as the ferromagnetic material, consisting of polycrystalline spherical particles with natural particle size distribution with an average particle size of 150  $\mu\text{m}$  (in Fig. 1 the particle size distribution is shown, measured by laser diffraction granulometer). The FeSi powder was mixed with Moplen HP501H polypropylene as the insulator, at a temperature of 240 °C for 15 min using HAAKE Rheolab Kneader. The mixed material was grinded and the resulting samples in the form of rings and cylinders were compacted by IM method (at a pressure approximately 280 MPa and a temperature of 240 °C). The ring-shape samples dimensions were: outer diameter 14 mm, inner diameter 10 mm, height 2 mm, and cylinder-shape samples: diameter 24 mm, height 2 mm. Composites with different volume content of polypropylene (25, 30 and 35 vol. %) were prepared, Tab. 1. The preparation procedure is shown in Fig. 2. The density and porosity of the composite materials were calculated from the mass and dimensions of the samples (FeSi density 7.85  $\text{g}/\text{cm}^3$ , polypropylene 0.9  $\text{g}/\text{cm}^3$ ), reaching values shown in Tab. 1. The porosity of the samples was achieved very low (< 0.5 %), which is an advantage of the IM method compared to the compaction using a press. On the other hand, there is a limit of IM for the maximum possible volume fraction of the ferromagnetic component of about 75 vol. % [1].

The microstructure of the samples is in Fig. 3(a,b) - observed with LOM, and in Fig. 4(a,b) - observed with SEM, showing FeSi particles in the polymer matrix. The structure of the composites seems to be isotropic and FeSi particles are homogeneously dispersed in polypropylene, which serves as good insulation coating for particles to be insulated from each other. This indicates high electrical resistivity of the composites.

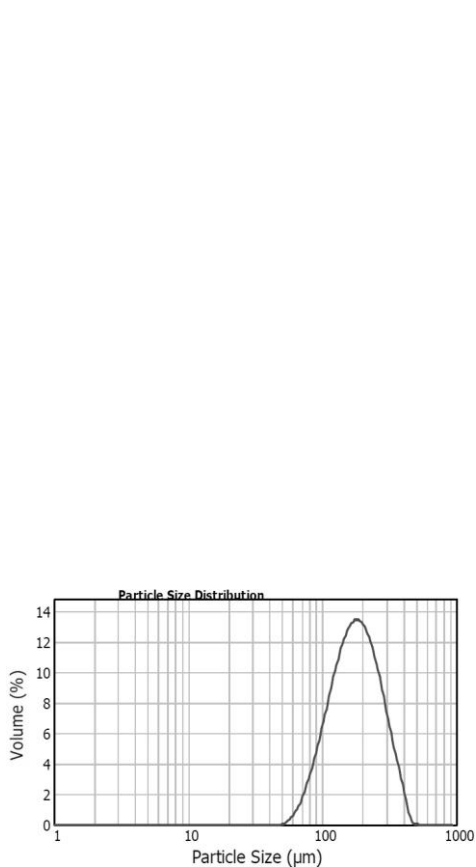


Fig. 1. Particle size distribution of the FeSi powder



Fig. 2. Preparation procedure of the FeSi-polypropylene composite samples, using injection molding

Tab. 1 Parameters of the FeSi-polypropylene composite samples

Sample	<b>FS150-25%</b>	<b>FS150-30%</b>	<b>FS150-35%</b>
FeSi powder to polymer ratio [vol. %]	75 : 25	70 : 30	65 : 35
Density [g/cm <sup>3</sup> ]	6.1	5.7	5.4
Porosity [%]	< 0.5	< 0.5	< 0.5

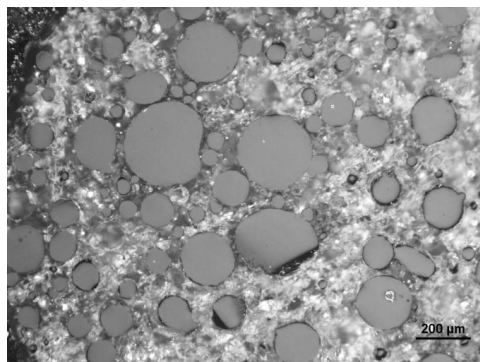


Fig. 3a Light optical microscopy image of FeSi particles in polypropylene matrix - sample FS150-35%

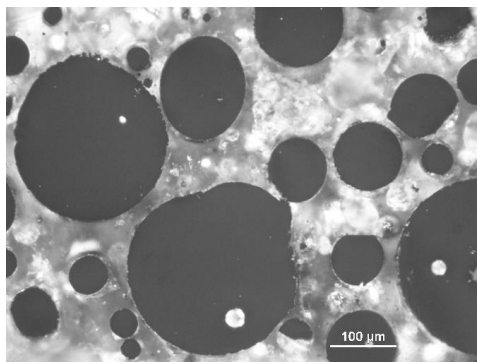


Fig. 3b Light optical microscopy image of FeSi particles in polypropylene matrix - sample FS150-35% (detailed view)

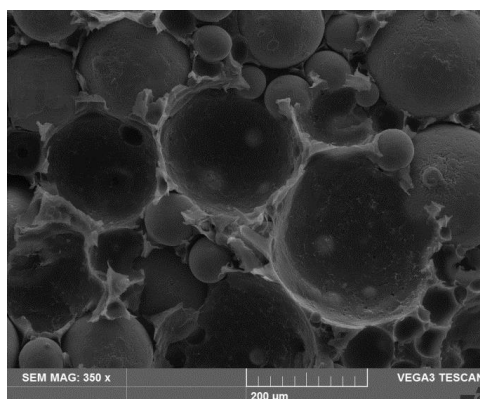


Fig. 4a Scanning electron microscopy image of FeSi particles insulated by polypropylene - sample FS150-25%

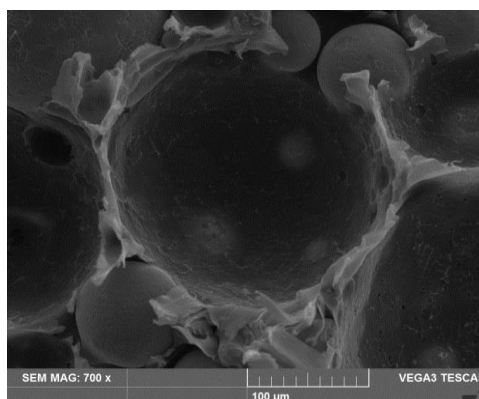


Fig. 4b Scanning electron microscopy image of FeSi particles insulated by polypropylene - sample FS150-25% (detailed view)

## ELECTRICAL AND MAGNETIC PROPERTIES

The specific electrical resistivity  $\rho_R$  was found to be beyond the range of the measurement device, i.e.  $> 10^4 \Omega \cdot m$  (Tab. 2), which is quite a high value for SMCs [3]. It is a result of good insulation of the conductive ferromagnetic particles by the polymer.

The coercivity  $H_C$  was found relatively low for SMCs (210-212 A/m), Tab.2. The values were near the value measured for the pure FeSi powder (190 A/m). It is assumed to be due to the relatively low and isotropic pressure applied during IM method, as well as the use of polymer insulation coating, ensuring the elimination of the internal stresses and deformations usually brought into ferromagnetic particles of SMCs at the compaction process [3,5-7].

The saturation magnetic flux density  $B_S$  was calculated as  $B_{S(FeSi)} \cdot C$  [12], where  $C$  is the filling factor (volume fraction of the ferromagnetic component) and  $B_{S(FeSi)} = 1.8 \text{ T}$  (value for FeSi powder with Si content of 6.8 wt. % [13]).  $B_S$  is increasing with the increasing ferromagnetic content in the composite, Tab. 2.

The maximum total relative permeability  $\mu_{tot}^{max}$  was obtained as the maximum of the total relative permeability  $\mu_{tot}$  calculated at the initial curve as  $\mu_{tot} = (B / \mu_0 H)$ , where  $B$  is the magnetic flux density and  $H$  is the magnetic field [13,14]. In Fig. 5 the initial magnetization curves referred to ferromagnetic component of FeSi-polypropylene composites with different polymer content are plotted. The steeper the slope of the initial curve is, the higher the permeability [13,14]. Values of  $\mu_{tot}^{max}$  show the increase with the increasing ferromagnetic content of the sample; the same is for the initial relative permeability  $\mu_i$ , Tab. 2.

The resonant frequency  $f_r$  was found to be very high, exceeding  $10^8$  Hz. At  $f_r$  the imaginary part of the complex permeability exhibits a peak and the real part drops to its half value.  $f_r$  is proportional to the specific resistivity of SMC [15], hence for these high-resistivity composites the high frequency stability was reached.

Tab. 2 Magnetic and electrical properties and parameters of the FeSi-polypropylene composite samples

sample	FS150-25%	FS150-30%	FS150-35%
Specific electrical resistivity $\rho_R$ ( $\Omega \cdot m$ )	$> 10^4$	$> 10^4$	$> 10^4$
Coercivity $H_C$ (A/m)	210	212	210
Saturation magnetic flux density $B_S$ (T)	1.35	1.26	1.17
Maximum total relative permeability $\mu_{tot}^{max}$ (-)	32	25.5	21
Initial relative permeability $\mu_i$ (-)	29	24	18.5
Resonant frequency $f_r$ (Hz)	$> 10^8$	$> 10^8$	$> 10^8$
Parameter $a_1$ (-)	0.07	0.01	0.04
Parameter $a_2$ (-)	1	1	1

The reversible relative permeability  $\mu_{rev}$  is defined as [14]:

$$\mu_{rev} = \frac{1}{\mu_0} \lim_{\Delta H \rightarrow 0} \left( \frac{\Delta B}{\Delta H} \right)_{H_1, B_1}, \quad (1)$$

where  $\mu_0$  is the magnetic constant,  $\Delta H$  and  $\Delta B$  are the magnetic field and the magnetic flux density increments when at each point  $[H_1, B_1]$  of the initial magnetization curve a small AC hysteresis loop is superimposed. The dependence of the reversible relative susceptibility  $\chi_{rev}$  ( $\chi_{rev} = \mu_{rev} - 1$ ) as a function of the magnetization  $M$  ( $M = (B / \mu_0) - H$ ) is different for different anisotropy in the material structure. For isotropic materials,  $\chi_{rev}$  can be described by the relationship [16,17]:

$$\chi_{rev} = \chi_i (1 - (M / M_S)^2), \tag{2}$$

where  $\chi_i$  is the initial susceptibility and  $M_S$  is the saturation magnetization. The general analytical expression involving any class of anisotropy has the form [18]:

$$\chi_{rev} / \chi_i = 1 - a_1 (M / M_S) - a_2 (M / M_S)^2 - (1 - a_1 - a_2) (M / M_S)^4, \tag{3}$$

in which the parameters  $a_1, a_2$  define the so-called structural anisotropy vector  $a = (a_1, a_2)$ . For predominantly anisotropic materials it is  $a_1 > a_2$  and vice versa, for predominantly isotropic materials it is  $a_1 < a_2$ . For example, in the case of anisotropic hardened steel 1018 the anisotropy vector (1, 0) was found, and for isotropic nickel-based annealed steel it was (0, 1) [18]. From the equation (3) we get for  $M \rightarrow 0$   $\chi_{rev} = \chi_i$  and for  $M = M_S$  (saturation state)  $\chi_{rev} = 0$ .

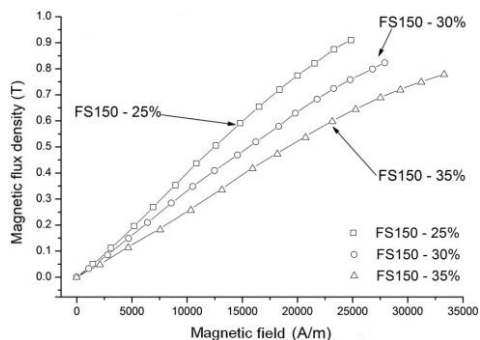


Fig. 5 Initial magnetization curves referred to ferromagnetic component of FeSi-polypropylene composites with different polymer content

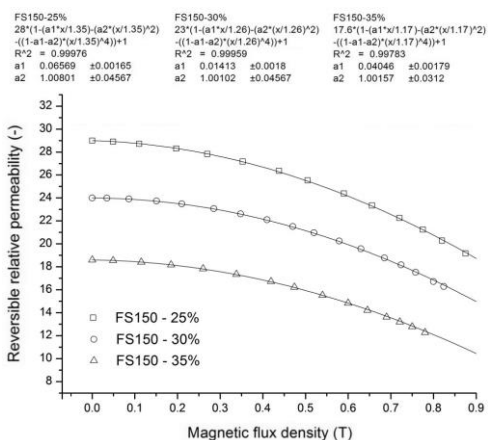


Fig. 6 Reversible relative permeability  $\mu_{rev}$  as a function of magnetic flux density  $B$  in ferromagnetic component of FeSi-polypropylene composites with different polymer content

In Fig. 6 the measured dependences of the reversible relative permeability  $\mu_{rev}$  as a function of magnetic flux density  $B$  in ferromagnetic component of FeSi-polypropylene composites with different polymer content are depicted. It was found that the given dependences can be described by the relation (3), which is generally valid for any structural anisotropy. The dependences were fitted with (3), using the relations  $\mu_{rev} = \chi_{rev} + 1$ ,  $\mu_i = \chi_i + 1$  and the approximate equality of ratios  $(M / M_S) \approx (B / B_S)$ . The obtained coefficients ( $a_1, a_2$ ) of the anisotropy vector are given in Tab. 2. It was found that in the investigated composite samples, when the parameter  $a_2 = 1$ , the parameter  $a_1$  shows only very low values close to zero, so that the structure of the samples can be considered almost completely isotropic. It is assumed to be the result of the IM preparation method, where the applied pressure is isotropic, unlike the uniaxial compacting by a press. The dependence of the parameter  $a_1$  on the polypropylene content was not observed.

## CONCLUSION

Soft magnetic composite materials composed of FeSi powder and polypropylene were prepared by the injection molding process. The volume content of polypropylene was 25, 30 and 35 %. The porosity of the composites was achieved negligibly low. Light optical and scanning electron microscopy revealed their isotropic structure and the homogeneous dispersion of FeSi particles in the polymer matrix. The visible good insulation of each ferromagnetic particle was proved by the high electrical resistivity of samples. The relatively low coercivity and sufficient saturation magnetic flux density and permeability values were reached. The high frequency stability (resonant frequency exceeding 100 MHz) of the initial permeability was observed. The fitting of the reversible relative permeability vs. magnetic flux density dependence with the general analytical expression for any class of anisotropy confirmed the structure of the composite samples to be isotropic.

## ACKNOWLEDGEMENT

This work was realized within the frame of the project “FUCO” financed by Slovak Research and Development Agency under the contract APVV-20-0072; and by Scientific Grant Agency of Ministry of Education of Slovak Republic and Slovak Academy of Science — projects VEGA 1/0143/20, VEGA 1/0225/20 and VEGA 2/0029/21. This work was also supported by the Development Operational Program Research and Innovation for the project “New unconventional magnetic materials for applications“, ITMS: 313011T544, co-funded by the European Regional Development Fund.

## REFERENCES

- [1] K.H.J. Buschow, Concise encyclopedia of magnetic and superconducting materials, Elsevier, Oxford, UK, 2005.
- [2] A.J. Moses, Advanced soft magnetic materials for power applications, in Handbook of magnetism and advanced magnetic materials, edited by H. Kronmüller and S. Parkin, Wiley-Interscience, New York, 2007.
- [3] E.A. Périgo, B. Weidenfeller, P. Kollár, J. Füzér, Past, present, and future of soft magnetic composites, *Appl. Phys. Rev.* 5, 031301 (37pp), 2018.
- [4] A. Schoppa, P. Delarbre, Soft magnetic powder composites and potential applications in modern electric machines and devices, *IEEE Trans. Magn.* 50, 2004304 (4pp), 2014.
- [5] K.J. Sunday, M.L. Taheri, Soft magnetic composites: recent advancements in the technology, *Metal Powd. Rep.* 72 (6), 2017.
- [6] M. Anhalt, B. Weidenfeller, Influence of filler content, particle size and temperature on thermal diffusivity of polypropylene-iron silicon composites, *J. Appl. Polym. Sci.* 119, 732-735, 2011.
- [7] T. Fiske, H.S. Gokturk, R. Yazici, D.M. Kalyon, Effects of flow induced orientation of ferromagnetic particles on relative magnetic permeability of injection molded composites, *Polym. Eng. Sci.* 37 (5), 826-837, 1997.
- [8] M. Anhalt, B. Weidenfeller, Dynamic losses in FeSi filled polymer bonded soft magnetic composites, *J. Magn. Magn. Mater.* 304, e549-e551, 2006.
- [9] B. Weidenfeller, M. Höfer, F.R. Schilling, Thermal and electrical properties of magnetite filled polymers, *Composites: Part A* 33, 1041-1053, 2002.
- [10] [www.hoganas.com](http://www.hoganas.com)
- [11] Birčáková Z, Kollár P, Füzér J, Bureš R, Fáberová M, Irreversible permeability and DC losses relationship for selected soft magnetic materials, *J. Phys. D: Appl. Phys.* 51, 395002 (10pp), 2018.
- [12] M. Anhalt, B. Weidenfeller, Theoretical and experimental approach to characteristic

- magnetic measurement data of polymer bonded soft magnetic composites, *J. Appl. Phys.* 105, 113903 (5pp), 2009.
- [13] D. Jiles, *Introduction to magnetism and magnetic materials*, Chapman & Hall London, 1994.
- [14] S. Chikazumi, *Physics of ferromagnetism*, second edition, Oxford University Press Inc., New York, 1999.
- [15] F. Mazaleyrat, L.K. Varga, *Ferromagnetic nanocomposites*, *J. Magn. Magn. Mater.* 215-216, 253-259, 2000.
- [16] C.S. Schneider, *Domain cooperation in ferromagnetic hysteresis*, *J. Appl. Phys.* 89, 1281-1286, 2001.
- [17] C.S. Schneider, *Maximum susceptibility of ferromagnetic hysteresis*, *IEEE Trans. Magn.* 48, 3371-3374, 2012.
- [18] C.S. Schneider, *Role of reversible susceptibility in ferromagnetic hysteresis*, *J. Appl. Phys.* 91, 7637-7639, 2002.



# SYNTHESIS OF Fe-BASED ALLOY REINFORCED WITH CHROMIUM CARBIDE VIA SINTERING OF IRON-FERROCHROME POWDER MIXTURE

Yevheniia Kyryliuk, Gennadii Bagliuk, Alla Mamonova, Vitaliy Maslyuk

## **Abstract**

*The results of the investigation of the structure, phase composition, and properties of the alloy sintered from a mixture of iron (65 %) and high-carbon ferrochrome (35 %) powders are presented in the article. It was shown that sintering of the consolidated specimens results in a substantially heterogeneous structure consisting of two predominant phases: austenitic phase and double ferrochrome carbide. A mechanism is proposed for the dissolution of ferrochrome particles in the iron matrix as follows:  $M7C3 \rightarrow M3C (1000\div 1150\text{ }^{\circ}\text{C}) \rightarrow M7C3 (1200\div 1250\text{ }^{\circ}\text{C})$ .*

**Keywords:** *powder, sintering, iron, ferrochrome, composite, phase composition, carbide*

## **INTRODUCTION**

Among the materials manufactured by powder metallurgy methods, wearproof materials occupy a significant place. The main requirement for ensuring high wear resistance of such materials is the need to create a heterogeneous structure consisting of a relatively soft matrix phase and hard inclusions of refractory compounds that significantly exceed the matrix material in terms of hardness [1,2]. It is obvious that it is just powder metallurgy technologies that make it possible to realize the basic conditions for the creation of wear-resistant materials of this type.

One of the promising groups of relatively inexpensive materials of this class is the composites consisting of an iron-based matrix phase with solid inclusions of chromium carbide [3-8]. These materials have shown high efficiency in operating conditions of intense friction, abrasive wear, corrosive environments, elevated temperatures, etc. The technology for their manufacturing involves the operations of joint grinding of steel and chromium carbide powders, compaction of the mixture, and sintering in the presence of a liquid phase [6-8].

In this work, we proposed the technology for the manufacturing of high-chromium heterogeneous sintered alloys, which is based on using high-carbon Fe-Cr master alloy (ferrochrome) powder instead of chromium carbide as a component of the initial powder mixture, which is designed to form a hard phase inclusions in the alloy. It was assumed that as a result of the interaction of the ferrochrome particles with the matrix phase at sintering temperatures, the corresponding carbide phase would be in situ synthesized in the alloy.

The goal of this work was to study the interaction of the mixture components and the features of phase and structure formation during the sintering of compacts from a powder mixture of iron with high-carbon ferrochrome.

## MATERIALS AND EXPERIMENTAL PROCEDURE

For the experiments, commercial powders of water-atomized Fe (200  $\mu\text{m}$ ) (Fig. 1(a)) and high carbon ferrochrome (100–200  $\mu\text{m}$ ), produced by mechanical grinding of lumpy ferrochrome (Fe-Cr) (Fig. 1(b)) were used. Ferrochrome contains 66.2 % Cr, 24.8 % Fe and 8 % (mass.) C.

A powder mixture with the ratio of 65% Fe - 35% (Fe-Cr) was prepared by wet ball milling in an alcohol medium, the overall nominal composition thus being Fe-23.2%Cr-2.8%C. Experimental specimens were produced by compaction on a hydraulic press at a pressure of 800 MPa. Samples of cylindrical shape with a size of 10×10 mm were prepared. To determine the physical and mechanical properties, samples in the form of a bar (5×5×35 mm) were prepared.

Sintering of the samples was carried out in a vacuum furnace in the temperature range of 1000–1300 °C with isothermal exposure of 30 minutes. The pressure in the vacuum furnace was  $1,33 \cdot 10^{-2}$  Pa. The density and porosity of the samples were estimated by the hydrostatic method in accordance with ISO 27.38.2009.

The morphology of the starting powders and the microstructure of the sintered materials were studied using optical (Olympus LX-70) and scanning electron (TESCAN VEGA) microscopes. The phase composition of the materials was determined on a Dron-3M diffractometer in Co-K $\alpha$  radiation. The sample during shooting rotated around its axis.

Local X-ray spectral analysis was carried out using an X-ray microprobe MS-46 from CAMECA (France). A quantitative analysis of the composition of the phases under study was made at points under the probe mode, an accelerating voltage of 20 kV, and a probe diameter of 0.7  $\mu\text{m}$ . The concentrations were calculated using the ZOND program [9], which was modernized according to the features of this work, which takes into account the above correction for absorption, fluorescence, and the atomic number of the element.

The microhardness of the structural components was determined on a PMT-3 device using a load of 0.49 N, and the strength properties of the material were determined using an INSTRON 8802 testing machine.

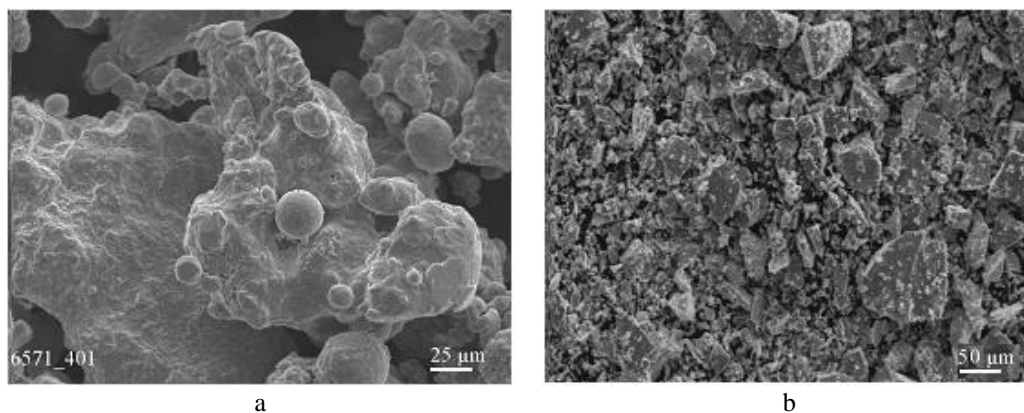


Fig. 1. Morphology of the starting powders of iron (a) and ferrochrome (b)

## RESULTS AND DISCUSSION

According to the micro X-ray diffraction analysis, high-carbon ferrochrome in a lump state consists of two phases (Fig. 2): double iron-chromium carbide with the composition: 10 % Fe - 80.6 % Cr - 8.9 % C (wt.) (Phase 1), and an iron-chromium-carbon alloy containing 72.7 % Fe - 22.3 % Cr - 4.8 % C (wt.) (Phase 2).

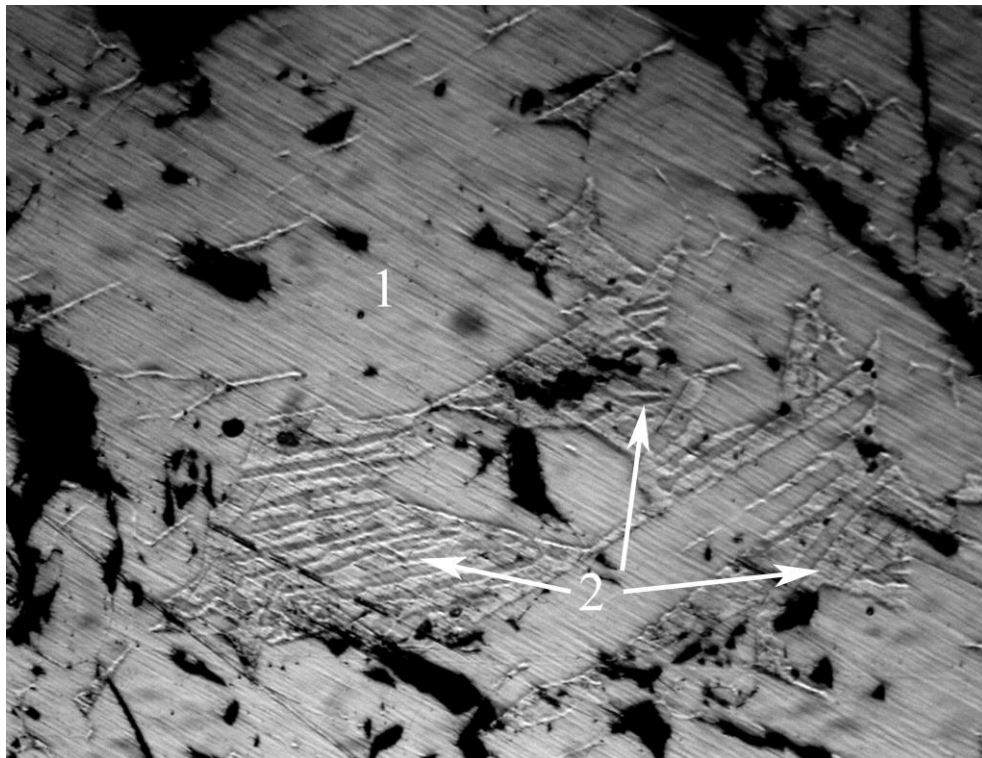


Fig. 2. The microstructure of the initial ferrochrome

The X-ray diffraction pattern analysis identified the phase composition of ferrochrome powder, which is presented by two main phases:  $(\text{Cr}, \text{Fe})_7\text{C}_3$  carbide and a solid solution of chromium in  $\alpha\text{-Fe}$ . In addition to the main  $(\text{Cr}, \text{Fe})_7\text{C}_3$  carbide component, weak intensity lines of  $\text{Cr}_3\text{C}_2$ ,  $\text{Cr}_7\text{C}_3$  carbides as well as  $\text{Cr}_{23}\text{C}_6$  with insufficient stoichiometry were detected, which is obviously due to the partial replacement of chromium by iron in  $\text{Cr}_{23}\text{C}_6$  carbide (Fig. 3).

Significant tailing of the (110) reflection of the ferritic phase indicates its nonequilibrium state, which is confirmed by the calculated values of the fine structure parameters. It was found that the physical broadening of (110) reflection is  $\beta_{110} = 14,5$  mrad, and the dispersion of the coherent scattering regions (CSR) is 15 nm.

The analysis of estimation of sintering temperature effect on structure and properties of sintered materials results showed that sintering at temperatures of  $1000\div 1100$  °C practically does not lead to shrinkage of the samples, while at the temperature of 1000 °C even some increase is observed (up to 1.5%) due to the Frenkel effect, which manifests

itself in the difference in the values of the heterodiffusion coefficients of chromium and iron in the powder mixture during sintering.

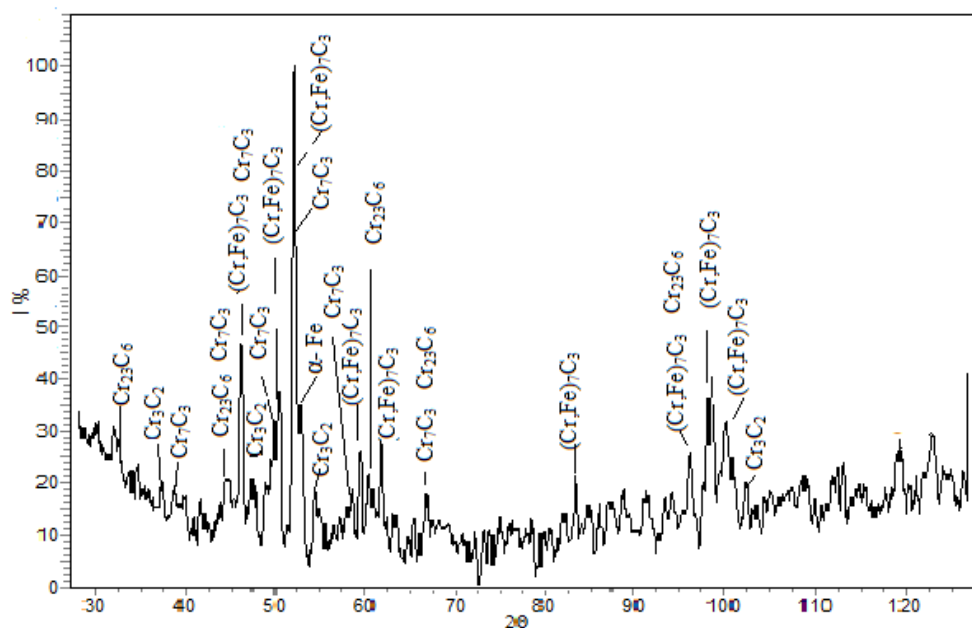


Fig. 3. The XR diffraction pattern of the ferrochrome powder

Slightly noticeable shrinkage of the samples occurs only at temperatures above 1150 °C, however, even sintering at 1200 °C does not provide samples of the material with minimal porosity. Only an increase in temperature up to 1250 °C allows obtaining samples with porosity not exceeding 2 %, while its increase to 1300 °C leads to partial melting and shape distortion of the samples.

The microstructure of the composite sintered at 1250 °C is essentially heterogeneous and consists of 2 predominant phases: dark gray, which is a double ferrochromium carbide, and a light gray metal component. A small number of pores (black) is observed on the microsection too (Fig. 4).

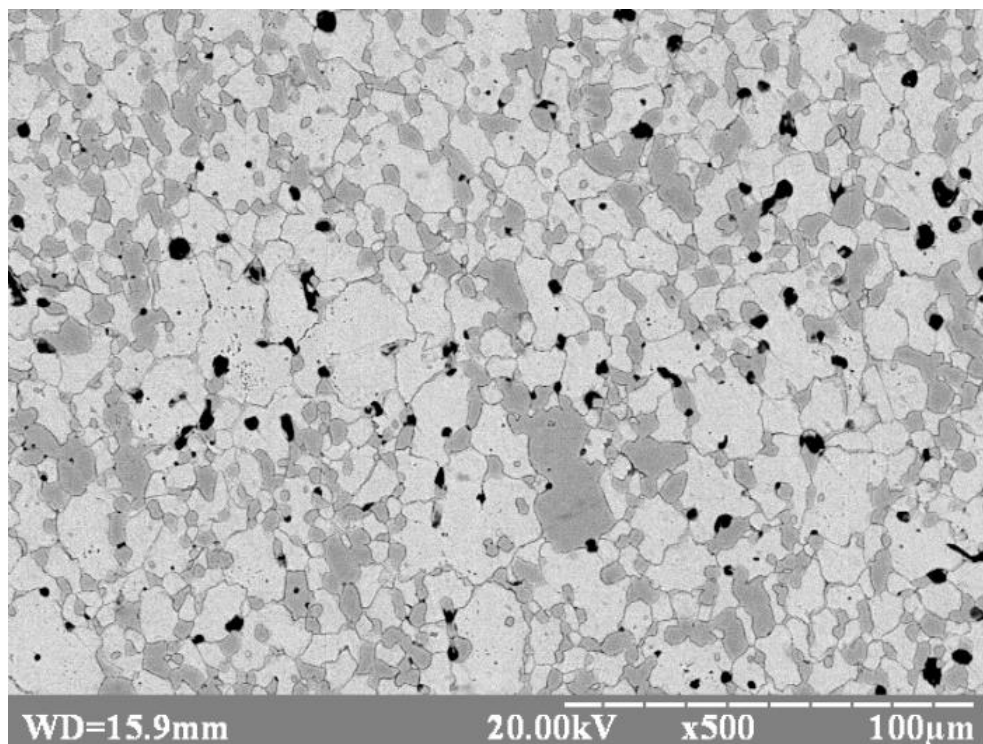


Fig. 4. The microstructure of the composite, sintered at 1250 °C

The estimation of the effect of sintering temperature on the microhardness of the matrix and main carbide phases of sintered composite (Fig. 5) made it possible to reveal the following regularities. With the increase of sintering temperature monotonic increase of matrix phase hardness is observed due to the thermally activated process of carbide transformations in the iron-ferrochrome system by the mechanism of chromium and carbon atoms diffusion from the main carbide phase of  $M_7C_3$  of ferrochrome into iron and counter flow of iron atoms to ferrochrome.

At the same time, the depletion of ferrochrome particles by chromium and carbon occurs, resulting in a sharp decrease in the microhardness of its carbides in the temperature range of 1000-1100 °C. However, with a further increase in sintering temperature to 1200–1250 °C, the reverse tendency is observed to increase in the microhardness of the secondary carbide phase formed based on the matrix phase.

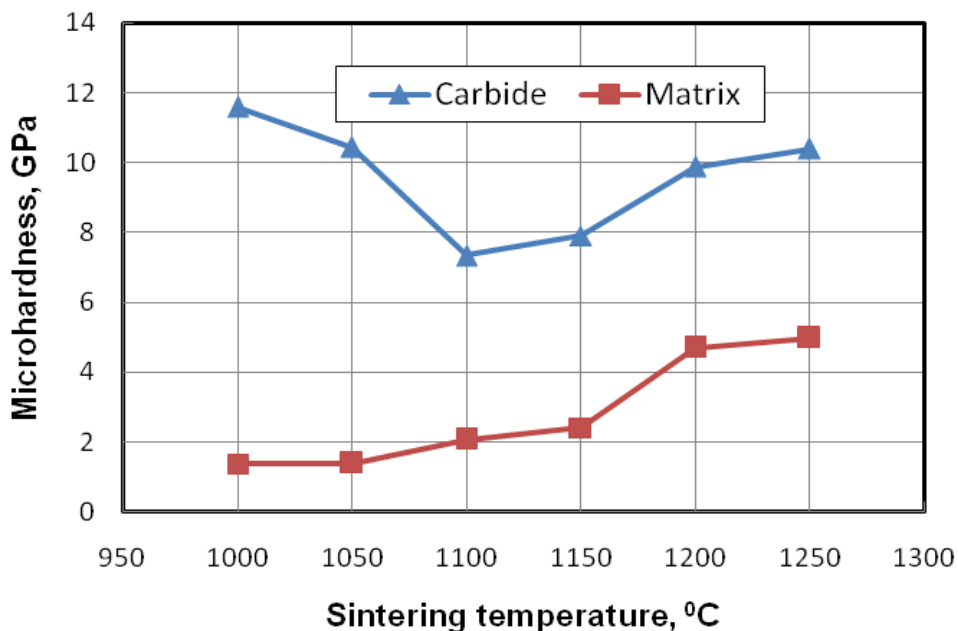


Fig. 5. The dependence of the carbide and matrix phases microhardness on the sintering temperature.

To establish the mechanism of this phenomenon, X-ray microspectral studies of the composition of the carbide phase of the composite sintered at different temperatures were carried out. According to these results (Tab. 1), sintering of compacts from a mixture of iron and ferrochrome powders in the low-temperature region leads to a certain decrease in the carbon content of the carbide phase from the initial 8.0 % (in ferrochrome) to 6.6÷7.1 % (wt.) after sintering at temperatures 1050÷1150 °C. At the same time, its atomic content decreases from 27.6 % to 25.1÷23.8 %, and the ratio  $C_c/C_m$  for atomic content of carbon (Cc) and metal (Cm) component of carbides decreases from 0.38 (in ferrochrome) to 0.31÷0.33. The data presented indicate the probability of execution of phase transformation of the initial carbide  $M_7C_3$  from ferrochrome, into  $M_3C$ .

Tab. 1. The effect of sintering temperature on elemental and phase composition of the carbide phase

$t, ^\circ\text{C}$	The content of elements in the carbide phase, % (mass./atomic)			$C_c/C_m$	Phase
	Fe	Cr	C		
20	69,2 /55,4	22,9 /17,1	8,0 /27,6	0,38	$M_7C_3$
1000	70,8/58,4	22,3 /17,1	6,9 /24,5	0,32	$M_3C$
1050	68,1 /56,6	25,3 /19,6	6,6 /23,8	0,31	$M_3C$
1100	68,3 /56,1	24,7 /18,9	7,1 /25,1	0,33	$M_3C$
1150	68,4 /56,2	24,6 /18,8	7,1 /25,1	0,33	$M_3C$
1200	67,7 /53,1	23,6 /17,2	8,8 /29,7	0,42	$M_7C_3$
1250	67,4 /52,1	23,5 /16,4	9,1 /31,5	0,46	$M_7C_3$

With the increase of sintering temperature to 1200-1250 °C, the diffusion intensity of chromium and carbon atoms from the main carbide phase of ferrochrome to iron increases, which becomes the basis for the formation of a new, secondary  $M_7C_3$  carbide phase. This fact is confirmed by the increase to 0.42÷0.46 of the value of the  $C_c/C_m$  ratio corresponding to the  $M_7C_3$  type carbide phase.

The above results allow us to present the mechanism of dissolution of ferrochrome in the iron matrix as the following sequence: at the first stage, in the temperature range of 1000–1150 °C at the interaction of ferrochrome particles with iron one-way diffusion of chromium and carbon from ferrochrome particles to iron occurs. It is accompanied by depletion of  $M_7C_3$  carbides located as a part of ferrochrome, by carbon and their conversion to  $M_3C$  carbides. With an increase of sintering temperature to 1200–1250 °C in consequence of recrystallization, new (secondary)  $M_7C_3$  carbides with a hexagonal lattice are formed in the alloy structure.

X-ray phase analysis of the composite sintered at 1250 °C showed (Fig. 6) that the most intense lines are fixed on the X-ray diffraction pattern, indicating the predominant presence of double carbide  $(Cr, Fe)_7C_3$  in the composition. The peaks of the  $Cr_7C_3$  and  $Cr_3C_2$  carbide phases,  $\gamma$ -Fe and  $\alpha$ -Fe are noted in the X-ray diffraction pattern too. It should be noted that  $\gamma$ -Fe and  $\alpha$ -Fe reflections, partially overlap with  $(Cr, Fe)_7C_3$  lines.

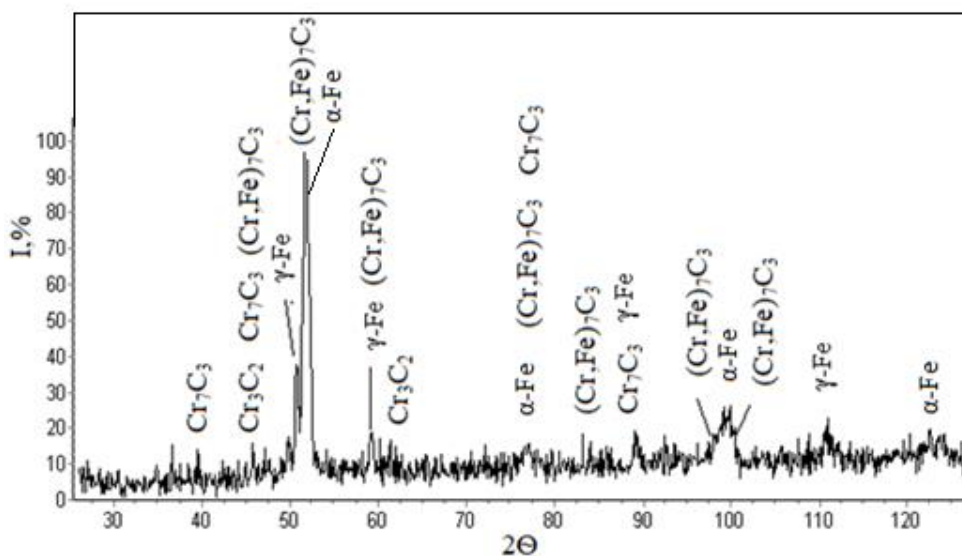


Fig. 6. The XR diffraction pattern of a sample sintered at 1250 °C

It can be assumed that during sintering of the mixture of iron and ferrochrome powders, part of the carbon from the carbide phase of high-carbon ferrochrome dissolves in Fe to form an austenitic phase.

The calculations of the fine structure parameters of the Fe matrix from the (111) and (311) profiles revealed a defect in the crystal lattice of the austenitic phase. Thus, the broadening of (111) line is  $\beta_{111} = 4.7$  mrad,  $CSR = 29$  nm. Profile (311) is characterized by broadening of  $\beta_{311} = 9.17$  mrad, microdistortions of the crystal lattice within  $9.0 \cdot 10^{-2}$ , and a dislocation density of  $\rho = 1.7 \cdot 10^{12} \text{ cm}^{-2}$ .

Tab. 2 shows the effect of sintering temperature on the Fe-35% FX800 properties. From the given data it can be seen that with an increase in the sintering temperature from 1100 to 1250 °C, the density of the samples monotonically increases, and the porosity decreases accordingly. The sintering temperature has a significant effect on the hardness of the composites and their bending strength. As can be seen from Tab. 2, with an increase in the sintering temperature to 1250 °C, the hardness and bending strength in the samples reach maximum values. This is explained both by a significant increase in sample density (decrease in porosity) and a possible strengthening of the adhesion bond at the carbide-metal matrix boundaries as a result of the more active interaction of the components. The best combinations of density, minimum porosity, and maximum hardness and bending strength of composites are observed at a sintering temperature of 1250 °C. The composite sintered at 1250 °C with a porosity of about 1.5÷2.5 % has a hardness of HRA 74÷75 and bending strength of 1760÷1900 MPa.

Tab. 2. The effect of sintering temperature on Fe-35% (Fe-Cr) properties

t, °C	$\gamma$ , g/cm <sup>3</sup>	Porosity, %	HRA	Bending strength, MPa
1100	7,1÷7,12	4,2÷4,4	55÷57	900÷1100
1150	7,14÷7,19	3,2÷3,9	68÷69	1150÷1280
1200	7,2÷7,22	2,8÷3	71÷72	1550÷1670
1250	7.25÷7,3	1,5÷2,5	74÷75	1760÷1900

## CONCLUSIONS

1. It is shown using the results of X-ray phase and X-ray diffraction pattern analyses, that during sintering of compacts from a mixture of iron powders and high-carbon ferrochrome, the components of the mixture actively interact with the formation of substantially heterogeneous structure.
2. The phase composition of sintered alloy includes the metal component which is a solid-solution austenitic phase and predominant content of double (Cr, Fe)<sub>7</sub>C<sub>3</sub> carbide.
3. The mechanism for dissolving of ferrochrome in the iron matrix is proposed as the following sequence: unilateral diffusion of chromium and carbon from ferrochrome particles to iron → depletion of M<sub>7</sub>C<sub>3</sub> carbides with their conversion to M<sub>3</sub>C carbide (at 1000÷1150 °C) → formation of secondary M<sub>7</sub>C<sub>3</sub> carbides with hexagonal lattice in consequence of recrystallization (at 1200÷1250 °C).

## REFERENCES

- [1] Fedorchenko, IM., Frantsevich, IN., Radomyselsky, ID., et al.: Powder metallurgy, materials, technology, properties, applications: Handbook. Kyiv: Nauk. Dumka., 1985, 624. (In Russian).
- [2] Baglyuk, GA., Poznyak, LA.: Powder Metall. Met. Ceram., vol. 40, no. 1, 2001, p. 34–39.
- [3] Lu, L., Soda, H., McLean, A.: Mater. Sci. Eng. A., vol. 347, Issues 1–2, 2003, p. 214–222.
- [4] Herranz, G., Matula, G., Romero, A.: Powder Metallurgy. vol. 60, Issue 2, 2017, p. 120–130.
- [5] Chang, CM., Chen, YC., Wu, W.: Tribol. Int., vol. 43, issues 5-6, 2010, p. 929–934.

- [6] Yakovenko, RV., Maslyuk, VA., Mamonova, AA., Gripachevskii, AN., Denisenko, NI.: Powder Metall. Met. Ceram., vol. 52, 2014, p. 644–650.
- [7] Yakovenko, RV., Maslyuk, VA., Gripachevskii, AN., Deimontovich, VB.: Powder Metall. Met. Ceram., vol. 50, 2011, p. 182–188.
- [8] Tolochin, AI., Laptev, AV., Yakovenko, RV., Maslyuk, VA.: Powder Metall. Met. Ceram., vol. 55, 2017, p. 518–529.
- [9] Tsikunov, NS., Batyrev, VA., Gripachevskii, AN. et al. A software package for processing the results of quantitative X-ray spectral microanalysis using the ZAF method on a mini-computer. Kyiv: Institute of Metallophysics, Academy of Sciences of the Ukrainian SSR. 1981, p. 40. (In Russian).



## **ANNOUNCEMENTS**

### **POWDER METALLURGY PROGRESS,**

an international open-access journal with 20 years of publishing history announces the

### **EXTENSION OF THE JOURNAL'S SCOPE**

Works from the fields of powder metallurgy, all powder-derived materials - metals, alloys, ceramics, and composites, basic and applied research of materials science related to mechanical and functional properties, manufacturing, and characterization are always welcomed.

But in 2021 the Scope of the Powder Metallurgy Progress will be extended to:

- materials research such as materials physics, materials chemistry, materials engineering, traditional and advanced powder metallurgy, materials processing;
- wide range of metal, ceramic and composite materials including metal matrix, ceramic matrix, polymer matrix composites, and hybrid organic-inorganic-metal-ceramic material systems, structural materials, functional materials, biomaterials, porous materials, magnetic electric and multifunctional materials such as magnetic composites, magnetoelectric, magnetocaloric, ferroelectric, piezoelectric, thermoelectric, magneto-optic, magnetostrictive, or high-temperature materials;
- advanced as well as traditional production technology and processing, additive manufacturing, 3D printing, Press and Sinter, HIP, MIM, PIM, Spark Plasma Sintering, Hot Pressing, Microwave Sintering, Plasma Treatment, Slip Casting, Rapid Heating, Ultrafast Sintering, new progressive compaction and processing methods;
- influence of material processing parameters on their microstructure formation and development and structural relations of physical, mechanical, and functional properties of materials focusing but not limited on powder materials;
- special technological processes of PM material with individual-particular-special physical-chemical properties;
- environmental issues of production and application of PM materials;

- industrial processes, management, and quality, (creation of normative) standard method activity, economical analysis, conception (philosophy) and prediction in PM and progressive material processing field;
- production of technological equipment for powder and advanced materials technology.

For more details visit the [PMP homepage](#).

# Call for PAPERS!



## POWDER METALLURGY PROGRESS

**AN INTERNATIONAL OPEN-ACCESS JOURNAL  
WITH 20 YEARS OF PUBLISHING HISTORY  
INVITES YOU TO SUBMIT MANUSCRIPTS FOR CONSIDERATION IN THE  
FORTHCOMING ISSUE OF THE JOURNAL.**



 PUBLISHED BY SCIENDO

 Find us on  
Facebook/PMProgress

## CONFERENCE ANNOUNCEMENTS

### 15<sup>th</sup> LOCAL MECHANICAL PROPERTIES CONFERENCE – LMP2022



*Dear colleagues,*

The 15th Local Mechanical Properties LMP2022 conference is planned to be held at the Institute of Materials Research of the Slovak Academy of Sciences in Košice, Slovakia, from Wednesday, May 11 to Friday, May 13, 2022., as a continuation of the successful meetings LMP from previous years (Košice 2004 and 2005, Plzeň – Nečtiny 2006, Brno – Šlapanice 2007, Herľany 2008, Telč 2009, Smolenice 2010, Olomouc 2011, Levoča 2012, Kutná Hora 2013, Stará Lesná 2014, Liberec 2015, Košice 2017 and Prague 2019).

The scope of the conference is traditionally focused on the results of research and development in the field of materials engineering, experimental methods, modeling, etc., with the aim to characterize the mechanical properties of materials from nano to micro/mesoscale. Contributions on indentation and other methods of hardness and other mechanical properties assessment, measurement of deformations and stresses, time-dependent properties with related microstructure analyses (TEM/SEM, FIB, AFM, etc.) regardless of material type (metals, ceramics, plastics, biomaterials, concrete, etc.) are welcome.

The conference will be held at the premises of the Institute of Materials Research of the Slovak Academy of Sciences in Košice. The possibilities for accommodation in Košice are indicated on the conference [website](#).

The conference language will be English. The conference will include invited lectures, oral and poster presentations. During the

conference, the participation of Ph.D. students in the LMP Poster Award competition is encouraged. The accepted contributions will be reviewed and published in the Special Issue of the journal [“Powder Metallurgy Progress”](#) which is an Open Access journal indexed by the Scopus database.

The early bird (prior to April 30, 2022) conference fee is 350 €, the regular fee is 380 €. For Ph.D. students, a reduced (early bird) fee of 250 € and 300 € (regular, after the deadline) are offered. The conference fee covers the organization of the conference, refreshment, and catering during the conference, gala-diner and social program, and the expenses for the publication of the accepted papers in a special issue of PMP journal.

Sponsors of the conference and exhibitors are welcomed.

Hopefully, the limitations on traveling and social contacts will be over by next November and LMP 2022 will provide again a possibility to re-establish the old to create new scientific and personal contacts, to gain and exchange knowledge and experience in a friendly atmosphere. Stay healthy and see you at LMP 2022 in Kosice.

František Lofaj  
Chair of the conference

#### **IMPORTANT DATES:**

- April 15, 2022 Abstract submission and registration
- April 30, 2022 Notification of acceptance
- April 30, 2022 Early bird conference fee payment
- May 5, 2022 Final program
- May 11-13, 2022 Manuscript submission and conference

## 7<sup>th</sup> INTERNATIONAL INDENTATION WORKSHOP



Over the last two decades, instrumented indentation became a standard method for probing the mechanical behavior of an extended range of materials at micro- and nano-scales in academia as well as in various engineering applications. Despite its wide acceptance in materials science, the technique still evolves and offers new possibilities. [The Seventh International Indentation Workshop \(IIW7\)](#) follows a series of international workshops on instrumented indentation devoted to the latest results of research and development in the field of instrumented indentation, its modeling, applications to materials engineering, and industrial applications. IIW conferences provide an excellent overview of the state-of-the-art in instrumented indentation, great opportunities to exchange new ideas in the advancement of this technique and its applications as well as to see the cutting-edge equipment by international manufacturers. The [scientific program](#) includes presentations by invited speakers, keynote speakers, regular presentations company presentations, and posters. The participation of young scientists in the Poster competition is encouraged.

IIW7 is organized by the Institute of Materials Research of the Slovak Academy of Sciences, in Kosice, Slovakia, and it will be held in the Congress Center at Smolenice Castle, Slovak Republic, from June 12, 2022, to June 16, 2022.

IIW7 will be held in the Smolenice Castle which is a Congress center of the Slovak Academy of Sciences. The Smolenice Castle is located at the foothills of the White Carpathian mountains near the village Smolenice, around 60 km from Bratislava and 80 km from Vienna airport. The castle was rebuilt on the ruins of medieval fortification in pseudo-gothic style at the beginning of the last century by Italian stonemasons.

The accommodation and catering will be provided directly in the castle. Please, note that the number of single-bed rooms is limited and room sharing among participants is anticipated.

## **INVITED SPEAKERS**

Prof. Dr. Mike Swain  
The University of Sydney  
Sydney, Australia

Prof. Dr. Gerhard Dehm  
Max-Planck-Institut für Eisenforschung GmbH  
Düsseldorf, Germany

Prof. Sandra Korte-Kerzel  
Department and Chair of Physical Metallurgy and Metal Physics,  
RWTH Aachen University, Germany

Dr. Finn Giuliani  
Department of Materials  
Imperial College  
London, UK

Dr. Verena Maier-Kiener  
Montanuniversität Leoben, Austria

Prof. Ruth Schwaiger  
Institute of Energy and Climate Research,  
Forschungszentrum Juelich GmbH,  
Juelich, Germany

## **KEYNOTE SPEAKERS**

Prof. Munawar Chaudhri

Prof. Upadrasta Ramamurty  
Prof. Dongil Kwon  
Prof. Jorge Alcalá  
Prof. Takeshi Ohmura  
Prof. Roberto Martins de Souza  
Dr. Kiran Mangalampalli  
Prof. Warren C. Oliver (G.M. Pharr, P. Pardhasaradhi)  
Prof. Yang-Tse Cheng

## **INTERNATIONAL ADVISORY COMMITTEE**

Jorge Alcalá, Universitat Politecnica de Catalunya, Spain  
Munawar Chaudhri, University of Cambridge, UK  
Yang-Tse Cheng, University of Kentucky, USA  
Nuwong Chollacoop, National Metal and Materials Technology Center,  
Thailand  
Sergey Dub, Institute for Superhard Materials, Ukraine  
Michael Griepentrog, Federal Institute for Materials Research and Testing,  
Germany  
Jae-il Jang, Hanyang University, Korea  
Nigel Jennett, University of Coventry, UK  
Ruth Schwaiger, Forschungszentrum Juelich GmbH, Germany  
Dongil Kwon, Seoul National University, Korea  
František Lofaj, Institute of Materials Research of SAS, Slovakia  
Jean-Luc Loubet, Ecole Centrale de Lyon, France  
Dr. Kiran Mangalampalli, SRM Institute of Science and Technology, India  
Christian Motz, Austrian Academy of Sciences, Austria  
Alfonso Ngan, University of Hong Kong, China  
Takahito Ohmura, National Institute for Material Science, Japan  
Upadrasta Ramamurty, Nanyang Technological University School of  
Mechanical and Aerospace Engineering, Singapore  
Roberto de Souza, University of Sao Paulo, Brazil  
Alexey Useinov, Technological Institute for Superhard & Novel Carbon  
Materials, Russia  
Chehung Wei, Tatung University, Taiwan

## LOCAL ORGANIZING COMMITTEE

Workshop chair	František Lofaj	IMR SAS, Kosice, Slovakia
Secretary	Lenka Kvetková	IMR SAS, Kosice, Slovakia
Members	Pavol Hvizdoš Ladislav Pešek Jiří Němeček	IMR SAS, Kosice, Slovakia TU Košice, Slovakia ČVUT, Czech Republic

## IMPORTANT DATES:

April 1, 2022	Abstract submission
April 15, 2022	Abstract acceptance notification
April 30, 2022	Early-bird registration & payment
May 31, 2022	Regular registration & payment
June 12-16, 2022	Conference

## BE A PART OF MAMC 2022!



**Ladies and Gentlemen,**

we have the pleasure to announce the

"7th Metal Additive Manufacturing Conference",

to be held September 26-28, 2022 in Graz (Austria).

We will continue the successful MAMC series of the Metal Additive Manufacturing Community.

Do not miss this opportunity to present your work at MAMC 2022 and submit your abstract as soon as possible.

The abstract submission deadline ends on *March 18, 2022*.

### **Topics:**

- Powder for MAM
- Systems & Equipments for MAM
- Additive Design & Engineering
- Laser Melting, Electron Beam Melting & Direct Energy Deposition Processes
- AM Process- and Quality Control
- Post-processing of AM parts
- Tools, Space and Aircraft, Automotive, Medical, and others
- Recent Research Topics

## **NEW: Metal Additive Manufacturing Start Up Award**

The award will be presented for the first time this year as part of the conference.

We are looking for great creative ideas, inventions, and developments, which are positively changing, influencing, and simplifying the process chain of Metal Additive Manufacturing.

Application Deadline: April 20, 2022

More information can be found under:

<https://www.mamc2022.org/start-up-award/>

Feel free to share information about this event with any person who is interested in the topics of Metal Additive Manufacturing.

*Also, do not miss the opportunity to become an exhibitor and sponsor of the conference to present your company!*

All information is available on our website:

[www.mamc2022.org](http://www.mamc2022.org)

We are looking forward to welcoming you in Graz!



**METAL  
ADDITIVE  
MANUFACTURING  
CONFERENCE  
2022**



**Call For Abstracts**

# Metal Additive Manufacturing Conference

*Industrial Perspectives in Additive Technologies*

**September 26 - 28, 2022**  
**Graz, Austria**

[www.mamc2022.org](http://www.mamc2022.org)

CONTACT: CONFERENCE SECRETARIAT  
 ASMET  
 Austrian Society for Metallurgy and Materials  
 Franz-Josef-Str. 18, 8700 Leoben, Austria  
 Phone: +43 3842 402 2290  
 Email: [mamc2022@asmnet.at](mailto:mamc2022@asmnet.at)

 **TU Graz**

 **ASMET**  
 THE AUSTRIAN SOCIETY FOR METALLURGY AND MATERIALS

©Fraunhofer ILT, Aachen / Volker Lannert

## Metal Additive Manufacturing Conference

**September 26-28, 2022**  
**Graz, Austria**

[www.mamc2022.org](http://www.mamc2022.org)

New:  
**Metal Additive Manufacturing**  
 Start Up Award 2022

### *Industrial Perspectives in Additive Technologies*

ASMET, the Austrian Society for Metallurgy and Materials, invites decision-makers, engineers, developers, industry experts, scientists and students to the 7<sup>th</sup> Metal Additive Manufacturing Conference with exclusive focus on the processing of metals.

- Powder for MAM
- Systems & Equipments for MAM
- Additive Design & Engineering
- Laser Melting, Electron Beam Melting & Direct Energy Deposition Processes
- AM Process- and Quality Control
- Post-processing of AM parts
- Tools, Space and Aircraft, Automotive, Medical and others
- Recent Research Topics

#### IMPORTANT DATES

Abstract submission: March 18, 2022  
 Notification of acceptance: April 15, 2022  
 Preliminary programme: April 22, 2022  
 Full paper Submission: August 26, 2022

 **ASMET**  
 THE AUSTRIAN SOCIETY FOR METALLURGY AND MATERIALS

**CONFERENCE CHAIRMAN**  
 Gerhard HACKL, ASMET

**SCIENTIFIC COMMITTEE**  
 Nader ASNAFI, Orebro University  
 Herbert DANNINGER, TU Wien  
 Franz HAAS, TU Graz  
 Christof SOMMITSCH, TU Graz  
 Jürgen Stampfl, TU Wien